

Original Article

# Experimental Investigations and Simulation of Solar-Powered Reverse Osmosis Water Desalination System using CFD

Shivaji S. Gadadhe<sup>1</sup>, Nilesh Diwakar<sup>2</sup>, Satish Chinchankar<sup>3</sup>

<sup>1,2</sup>Department of Mechanical Engineering, School of Engineering, SSSUTMS, Sehore, M.P.(India)

<sup>3</sup>Department of Mechanical Engineering, VIIT, Pune (India)

<sup>1</sup>Corresponding Author: [shivaji.gadadhe@gmail.com](mailto:shivaji.gadadhe@gmail.com)

Received: 14 September 2022

Revised: 09 February 2023

Accepted: 25 February 2023

Published: 25 April 2023

**Abstract** - In this article, a solar-powered RO desalination system is investigated and simulated in detail. A solar PV panel with a negative temperature coefficient will have a lower efficiency as the temperature increases. The average photovoltaic (PV) solar panel has a conversion efficiency of 6-18 percent, which means that 84-96 percent of the energy that is produced is wasted. When recovering energy from solar PV panels, it is possible to collect more thermal energy than the electrical energy that the PV panels themselves supply. The heat was transferred from the panel's top and bottom by directly contacting moving water at both locations. PV panel performance and energy recovery were both increased via direct contact heat exchange from the panel's top surface. The incident radiation is made more straight when light is refracted by water. Increasing the angle of radiation and maintaining a cooler panel temperature both enhance solar efficiency. The CFD modeling of the temperature of PV panels matched the actual results. Large-scale solar photovoltaic (PV) systems are able to recover more energy. Therefore, the present research implies that the panel's performance may be improved by controlling its temperature and collecting thermal energy for use in other applications.

**Keywords** - Reverse Osmosis, Solar photovoltaic, Refraction of Light, CFD.

## 1. Introduction

By forcing the water to go through semi-permeable membranes in a process known as "reverse osmosis," salty ocean water may be transformed into freshwater. Because the membrane in reverse osmosis is a thin film composite made of nonwoven polyester, polysulfone, and a polyamide barrier layer, it can remove salts, bacteria, and viruses in addition to suspended particles. This makes it feasible for the process to remove suspended solids. Because pressure is the driving force behind water movement, the membrane process has to make use of energy in order to produce water. This is because the pressure is the driving force behind water flow.

As a consequence of this, facilities that use the process of reverse osmosis need a trustworthy source of power supply in order to operate effectively. Solar-powered reverse osmosis plants are an intriguing possibility for constructing plants in remote regions of developing countries with unreliable access to electrical power supplies but located in regions endowed with high solar radiation intensity, such as the arid tropics. One of the most promising solutions for decreasing greenhouse gas emissions and for stand-alone reverse osmosis systems in rural and remote places is solar-powered reverse osmosis, which has been regarded as one of

the most promising technologies. In the preceding ten years, reverse osmosis has matured into a well-established technology that has been successfully implemented in a variety of locations around the world. This development occurred mostly in the United States.

On the other hand, the quantity of energy necessary to produce water has continued to be a major cause for concern. In order to manufacture freshwater from saltwater and brackish water, respectively, water treatment facilities need around 3-4 kWh of energy for every cubic meter of feed water. The total dissolved solids level of the feed water may significantly impact the quantity of energy that must be used.

## 2. Literature Survey

This section contains a few articles that were chosen for an in-depth analysis to find a research gap or further extend the research already done in the field of hard turning. The following is a list of the articles that were chosen for the study:

Aburub, A., et al. (2017) [1] "presented the performance of water-heated, cross-flow humidification dehumidification (HDH) desalination system with brine recirculation designed,



constructed, and operated in a controlled environment. They introduced HDH devices that were simple to construct, simple to maintain, and ideal for distant places with little technical expertise. The impact of mass ratio (MR) on GOR, RR, humidifier, and dehumidifier efficacy was studied. The system was tested at 60-75 °C hot water temperatures and 4-18 L/min hot water flow rates. The developed system can produce 92 liters of distillate water per day, has a GOR of 1.3, and the component efficacy ranges from 92–97 percent for a dehumidifier and 53–79 percent for a humidifier”.

Ahmad, N., et al. (2015) [2] “presented analytical modeling and simulation with experimental verification of photovoltaic system driving reverse osmosis water desalination. In a photovoltaic system, the influence of fixed and tracking PV panels on collected insolation and PV power was studied. The RO division created a full membrane model that predicts feed water pressure and permeates flow rate. The proposed PV and RO models were verified by experimental data singly and together (combined PVRO). Using this verified model, the influence of PV panel slope and azimuth angle on permeate flow rate was explored year-round. The clean water flow rate increments for annual tilt, monthly tilt, and single and double-axis tracking PV panels are determined. A year-round ideal tilt angle of PV panels due south was close to 0.913 times Dhahran's latitude. Annual permeate gain with annual optimum tilt and monthly optimal tilt of PV panel installation vs to flat panel installation was 10% and 19%. Using single and dual-axis tracking systems, the PV orientation (tilt angle and azimuth angle) may be adjusted. The annual permeate gain of single and double-axis continuous tracking PV panels is 43% and 62%”.

Ahmed, F. E., et al. (2019) [4] “discussed the most recent developments in photovoltaic powered reverse osmosis (PV-RO), solar thermal powered reverse osmosis (ST-RO) with respect to membrane materials, process configuration, energy recovery devices, and energy storage. Globally, desalination capacity has increased significantly to meet rising water demand. The focus has switched to employing renewable energy sources to reduce the carbon impact of high-energy desalination procedures. Sun-powered desalination offers a sustainable answer to water shortages in locations with abundant solar irradiation. The compatibility of any desalination process with solar technology is determined by the kind of energy required and its availability. Because photovoltaic and solar thermal solar energy technologies are rapidly developing, there is considerable interest in linking solar energy with desalination to improve energy efficiency. Also covered were recent developments in sun-powered membrane distillation (MD) and still solar materials. The future forecast involves solar-powered forward osmosis and evaporation. The technology and energy usage of solar-powered desalination devices has been studied”.

Alghoul, M. A., et al. (2016) [5] “quantify the effect of climatic-design-operation conditions on the performance and durability of a PV-BWRO desalination system. Small-scale brackish water reverse osmosis (BWRO) desalination facilities are less profitable than large-scale ones. Integrating renewable energy systems with small-scale units might hypothetically help their commercialization. In reality, RO units are modular, allowing them to adapt to renewable energy sources. Small-scale PV-RO desalination systems might be useful in distant places where BW is more widespread. A 6-month small-scale unit is developed, built, and tested. Only a 2 kWp PV system with five membranes, a feed TDS of 2000 mg/l, and a permeate TDS of 50 mg/l were allowed. Data on solar radiation and temperature were studied to establish their impact on the unit's present and future activities. A two-stage design was shown to be optimal for 600 W RO load, membrane type, and design configuration. The PV system was able to provide the load while the RO unit maintained steady permeate flow and salinity. Using the PV-BWRO system for 10 hours would create 5.1 m<sup>3</sup> of fresh water at 1.1 kWh/m<sup>3</sup>. There are several hours of high temperatures during PV module operation (over 45°C) and battery room conditions (above 35°C), both of which might significantly affect power output and battery autonomy. Optimum thermal management of PV module and battery bank room conditions is vital in maintaining optimal operating temperatures”.

Ali, E. S., et al. (2017) [7] “investigated the effect of reverse osmosis brine recycling employing adsorption desalination on overall system desalinated water recovery. The input, pretreatment, and brine disposal costs of reverse osmosis seawater desalination systems account for around 25% of the overall cost. Adsorption desalination creates high-quality drinkable water and a cooling effect. The brine from the RO system feeds the adsorption desalination system. Low-temperature heat sources like solar energy power it. MATLAB triggered the adsorption desalination system. The suggested combination approach improves recovery while decreasing permeate salinity. Aside from improved system performance, a cooling effect is created, that may be used for cooling”.

Ali, I. B., et al. (2014) [9] “investigated systemic modeling of a small-scale Brackish Water Reverse Osmosis (BWRO) desalination unit. This device was powered by a photovoltaic-wind hybrid system with no batteries. The RO desalination process involves mechanical, hydraulic, chemical, and thermal fields. Thus, this study proposes an interdisciplinary strategy. The bond graph is a well-known dynamic modeling tool for such a multi-physical system. A BWRO test bench is characterized experimentally to evaluate the developed bond graph model of the examined desalination process. The simulation findings show considerable results when compared to the experimental results”.

Antar, M. A., et al. (2013) [11] “conducted experiments on a single- and two-stage air-heated humidification–dehumidification desalination system (HDD) driven by solar energy. The system is located in Dhahran, Eastern Province, Saudi Arabia. Natural water sources are scarce in this environment. Desalination is being used in Saudi Arabia. It is the global leader in desalination. Modern desalination facilities use fossil fuels and require a lot of electricity. Since the region has an abundance of solar energy, efforts are undertaken to use solar energy to provide fresh water for distant places. It has been noted that HDD systems may effectively provide fresh water in isolated regions where pipeline access is difficult. The technology employed in this research is a solar-heated closed-water closed-air cycle with a single or two-stage operation. The air is heated using evacuated tube sun heaters. In a humidifier, warm air is sprayed with salt water in a countercurrent direction. When using the two-stage system, additional heating and humidification processes occur. The humidified air is subsequently dehumidified using water (condenser). The dehumidifier air is recirculated to the solar heaters. The dehumidifier's water cycle is split in two due to the water's high temperature. The first cycle sends water from the cooling water tank to the condenser and back to the tank. On the other, water is pumped from a tiny tank to humidifiers and sprayed. The rejected brine goes back in. The tiny tank keeps the cycle water warm by interacting with hot humidifier air. A float valve connects a makeup tank to this tank to compensate for evaporating water. Sensors in the system detect dry and wet bulb temperatures, flow rates, and solar radiation flux”.

Ayav, P. İ., et al. (2007) [12] “presented a theoretical and experimental study of solar distillation in a single basin constructed at İzmir Institute of Technology Urla Campus. The world demand for potable water is increasing steadily with a growing population. Desalination using solar energy is suitable for potable water production from brackish and seawater. The still has a base area of 2100 mm × 700 mm with a glass cover inclined at 38°. In order to obtain extra solar energy, an aluminum reflector (2100 mm × 500 mm) is also assembled to the still. They model the still and conduct its energy balance equations under minor assumptions. They consider the temperatures of the glass cover, seawater interface, moist air, and bottom in theoretical calculations and measurements. The comparison of the theoretical and experimental results highlights the benefits of the proposed model of the still and the efficacy of its energy balance equations”.

Buragohain, S. et al. (2020) [14] “installed A pilot-scale 1 kW photovoltaic (PV) system at Auniati Satra near IIT Guwahati for studying the effects of its operating parameters at different loading conditions corresponding to the environmental conditions prevalent in Guwahati, Assam (India). To fulfill rising load needs, decentralized energy

production at the community level is required. During the day, the PV system was exposed to eight different loading conditions: 20%, 30%, 40%, 50%, 60%, 70%, and 80%. Insolation, PV energy, PV charge, temperature, and battery capacity data were analyzed hourly. The optimal loading condition in stand-alone mode is 45-50 percent load with normal solar insolation and may be increased to 70 percent throughout the day with high solar insolation. In grid-connected mode, up to 45% of load applications saved money by reducing power use from the local grid. The ac supply may expose it to virtually full rated capacity”.

BURGAÇ, A., et al. (2021) [15] “investigated both ambient conditions and the design parameters. The study contributes to determining variation in the specific power consumption and related total power requirement of the single-stage reverse osmosis desalination plant model with the ambient conditions and design parameters. Humanity's most pressing necessities are clean water and electricity. The growing population and the demand for freshwater make desalination a hot subject. One prominent desalination method is reverse osmosis. Reverse osmosis has a lower energy usage than conventional desalination procedures and is more resistant to feedwater salinity. The ambient conditions are crucial factors determining desalination efficiency.

Conversely, the design specifications of a reverse osmosis desalination plant are crucial. For power needs, design characteristics and ambient circumstances are discussed in the findings. The simulations are run at a constant manufacturing rate to evaluate how each parameter affects product attributes. Increased seawater temperature reduces electricity usage while increasing end-product salinity. The findings showed that design parameters should be tuned for system size and feedwater salinity”.

Marmara, Turkey. Chaaben, A. B., et al. (2011) [17] “studied a new modeling approach of a small photovoltaic reverse osmosis (PV-RO) desalination unit. The suggested model treats the unit as a MIMO process. The most extensively used desalination technology is reverse osmosis (RO), used to desalt saltwater and purify brackish water. Using these methods necessitates a control system. As a result, a dynamic system model with experimental validation is required. An empirical transfer matrix shows the relationships between the output and input variables. The unit has a state model. Several experimental data validate the suggested model. As a consequence, the unit model may be simply utilized to create a process control loop to ensure optimal operating conditions and decrease water production costs”.

Chaker, R. et al. (2010) [18] “presented a Photovoltaic (PV) simulation system powering reverse osmosis (RO) desalination unit with no energy recovery device (ERD).

Transient System Simulation (TRNSYS®) is used to simulate the system. The PV system comprises 55 W solar panels coupled to a storage battery through a DC-DC charge controller. A pump supplies feed water to the RO system. Contains one Filmtec spiral wound membrane. The simulation results for freshwater production revealed a total capacity of 110 m<sup>3</sup> per year with a continuous input of 1.5 m<sup>3</sup>h<sup>-1</sup>. The monthly freshwater production grows with increasing raw water input flow and PV surface. They also found that when raw water salinity increased, so did freshwater production. This study is supported by experimental findings”.

Chen, C., et al. (2019) [20] “discussed the water resources and solar energy utilization status in China and presented a comprehensive review of a possible solution: coupling desalination technologies with sustainable energy. Freshwater and energy are the two main problems for human life and sustainable growth. China's massive population requires a lot of fresh water. To provide a steady supply of clean water, desalination is an intelligent and promising technique. However, excessive energy usage and greenhouse gas emissions have hampered desalination growth. Solar energy is unique in that it may be used in many ways. The desalination market in China is analyzed, and energy consumption for various desalination procedures is outlined. We compare two solar-powered desalination technologies. This research will assist China's desalination sector in moving from traditional energy sources to solar-powered desalination”.

Cherif, H., et al. (2011) [21] “elaborated the energy and water production estimation on a large-scale time from a Photovoltaic–Wind hybrid system coupled to a reverse osmosis desalination unit in southern Tunisia. Hybrid desalination systems promise to be a potential alternative for isolated and desert places. The energy is utilized to make drinkable water. These include wind speed, solar irradiance, and steady-state models. The findings reveal that the hybrid system (solar and wind) provides year-round energy availability, despite day, season, and year variations. The reverse osmosis desalination machine driven by a Photovoltaic–Wind hybrid system is suitable for southern Tunisia (salinity 6 g/l). The Djerba region's brackish feed water compositions were chosen. Double-stage desalination employing spiral modules is widely utilized, and steady-state model validation is shown”.

As a result of reading the review, we may get the conclusion that scientists have experimented with cooling solar panels. In spite of the significant amount of research that has been done on solar PV panel heat transfer, there is still a research gap in the modeling and experimental validation of heat transfer with water cooling from the top surface. The present study examines the heat transfer characteristics of solar panel cooling with the goals of

increasing panel efficiency and constructing a deeper understanding of energy recovery.”[21]

### 3. Experimentation

Heat transfer from solar photovoltaic panels provides a challenge, which should be addressed by increasing the panels' efficiency. Since this is the most effective technique to enhance heat transmission, the panel should have no obstructions in the path of incoming solar radiation, and there should be nothing above it. As a result of the fact that radiations originate from the top, a direct contact heat exchanger system with water serving as the coolant was developed. The heat exchange was designed to bring the solar panel's temperature down to an acceptable level. Insulation made of calcium silicate was used to successfully insulate all of the panel's surfaces, including the back and each of its sides. The objective was to boost the efficiency of the photovoltaic conversion process while maximizing the amount of thermal energy that could be used, decreasing the amount of thermal energy that might be wasted, and doing so as little as possible.

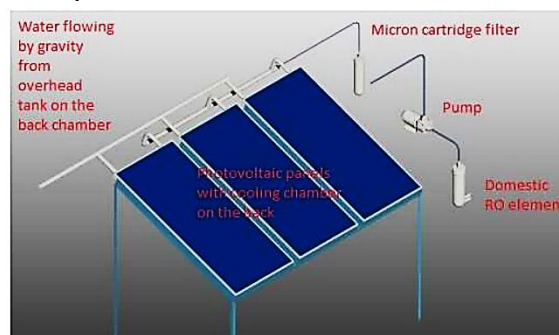


Fig. 1 Experimental Unit

#### 3.1. Materials

Solar photovoltaic panel with a power output of 70 watts, an aluminum frame, a rheostat, a water tank, thermocouples, and a pyranometer.

#### 3.2. Method

At the location in Pune, India, the solar panel was angled toward the south at a 20-degree angle, as can be seen in Figure 1. This was done to ensure that the panel received the most amount of sunlight possible (coordinates: 21.7600 0N and 72.1500 0E). In order to get the possible advantage from the sun's beams, this was carried out. While one of the photovoltaic (PV) panels were cooled by having air forced down on it from above, the other panel was not cooled in any way. With the assistance of the variable resistance system, also referred to as a rheostat, the V-I (voltage-current) performance of the solar panel was measured and analyzed. As seen in Fig.1, the system that enabled cooling to be provided from the top was comprised of a pipe perforated throughout its length at the top, with the holes having a diameter of 2 millimeters. This pipe was positioned at the top of the structure. We examined the solar panel's V-I performance while increasing the cooling water's flow rate

from 1 liter per minute to 2 liters per minute. The water that was gathered at the exit was poured into a tank that was exposed to the air, and it was then recirculated with the assistance of a DC (direct current) Kemflo pump. This process was repeated until all of the water had been used. The pump's average flow rate was one liter per minute for each hour it was in use. Two pumps are used here since the desired flow rate is 2 liters per minute for each individual pump.

#### 4. CFD Simulation

The simulation of this model was carried out with the help of the ANSYS Computational fluid dynamics program. The following diagram illustrates the assumptions that were made while modeling the system using the ANSYS CFD tool.

- It is assumed that the height of the water layer above the panel is always 2 millimeters.
- The rate of flow is consistent.
- The temperature of the water changes as time passes (Water absorbs the solar radiation).
- The proportion of infrared radiation to total incident radiation is fifty percent, whereas that of visible radiation is forty percent, and that of UV radiation is ten percent.
- A substance that is opaque has an absorptivity of 80 percent.
- Glass has a transmittance of 80 percent, an absorptivity of 20 percent, and no reflection at all.
- Pipe material does not absorb radiation.

In order to ensure that the solution would eventually converge, simulations were run using the ANSYS CFD program with boundary conditions being applied. The following distinct layers make up the solar panel; Table 1 provides information on the features of each layer that pertain to its physical makeup.

**Table 1. Physical characteristics of the components that make up a PV panel**

Layer	Thickness t (m)	Thermal Conductivity (w/mK)	Density (kg/m <sup>3</sup> )	Specific Heat Cp(J/kg K)
Tedlar	0.0001	02	1200	1250
Rear contact	10 x 10 <sup>-6</sup>	237	2700	900
EVA	500 x 10 <sup>-6</sup>	0.35	960	2090
PV Cell	225 x 10 <sup>-6</sup>	1.48	2330	677
ARC	100 x 10 <sup>-9</sup>	32	2400	691
Glass	0.003	1.8	3000	500

Because the feed water pipe has holes, the panel's geometry had to be designed with eight inlets and four outputs of water flowing from the panel. This was done by imagining the panel to have a square shape. It has been

ensured that the air domain, which incorporates the physical geometry, is taken into account. After that, the geometry was constructed by considering one slit-type entry and one outflow to recreate the conditions of the experiment. Fig.2 displays a system's meshed domain with 8 inlets and 4 outlets. There is no skewness or orthogonal quality in the mesh; it has a value of 0 in both categories.

#### 5. Result and Discussion

The first part of this section discusses the findings of systems with 8 inlets and 4 outlets. In the latter portion of this section, a simulation of the system is performed using just one inlet and one exit. Fig.3 shows the outline of the model's structure.

Fig.4 illustrates simulation results for back and top panel temperatures. Due to rear insulation, heat cannot escape. On the back, the average temperature is approximately 36°C, except at the lowest corner, where it reaches 60 °C. The lowest corners of the panel, where water cannot flow, are hotter than the top, where it is 27 °C. Cooling from the top cools the array surface, and insulation minimizes heat loss. The cooling is successful since the rear surface temperature is not too high.

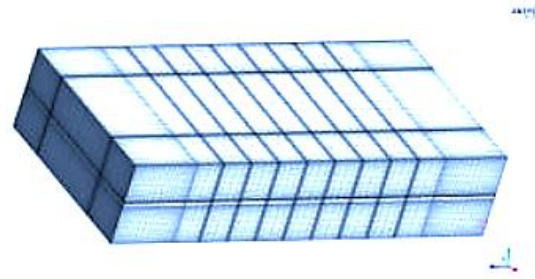


**Fig. 2 Mesh domain with eight inlets and four exits in the system**

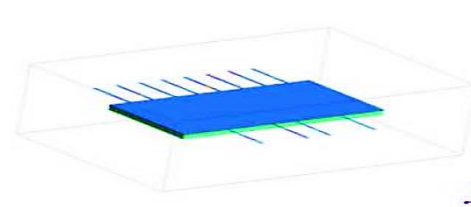


**Fig. 3 An outline of the model's structure**

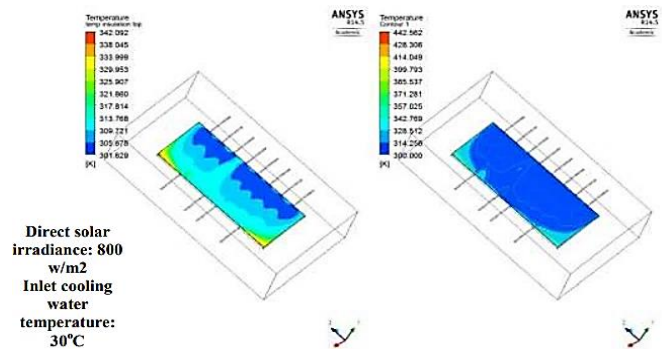


**Fig. 4 Temperature of the rear surface of the solar panel as well as the top surface**

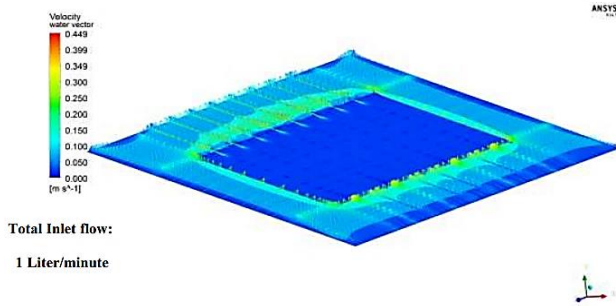


Fig. 5 Velocity of water over the photovoltaic panel

The speed of the water as it passes over the solar panel is seen in Fig. 5. Over the panel, the velocity is minimal, coming in at less than 0.05 meters per second, but it is much greater at the entrance and exit sites. The velocity profile is shown on a photovoltaic panel that makes up the middle section of the structure. The solar panel's temperature, shown in Fig.6, demonstrates that this velocity was sufficient to adjust the temperature to the desired level.

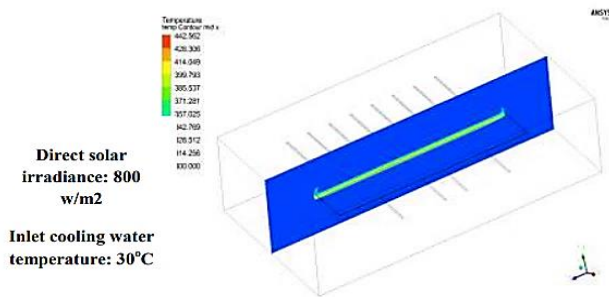


Fig. 6 Temperature measured at the intersection of two solar panels.

The solar panel's temperature can be seen across the cross-section in Fig.6. Insulation has a direct role in the temperature rise experienced at the structure's base, as is made abundantly clear. It makes sense that the temperature of the rear side would rise when thermal energy is supplied from the top, but it is not permitted to leave from the bottom. This would cause the temperature of the backside to rise. The insulation does a good job of preventing heat from escaping, and the heat moves downward from the source.

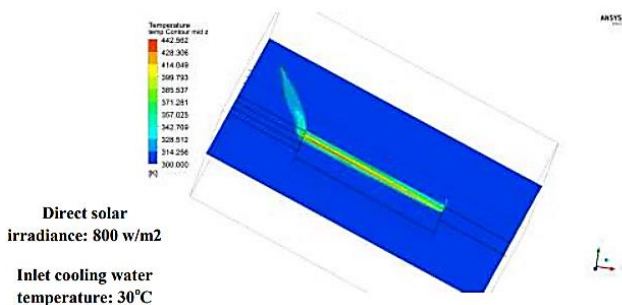


Fig. 7 The temperature at which a solar panel's cross-section is measured along the z-axis.

The temperature of the cross-section along the z-axis of the solar panel is shown in Fig.8. The natural convection of air that occurs above the panel is the reason for the fluctuating temperature.

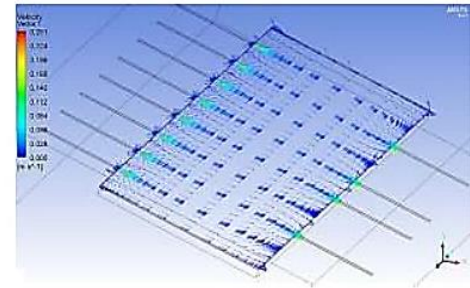


Fig. 8 The velocity vector over the surface of the PV panel.

The velocity vectors above the solar panel's surface are shown in Fig. 9, which may be seen here. The velocity at the entry, as well as the velocity at the outflow, has both greatly risen. The pressure is lower at the exit because the flow is focused on a smaller opening than at the entry, where the flow is also concentrated on a smaller opening. There were a lot of holes or perforations all the way down the length of the pipe. As a result, in order to mimic the actual experimental situation with a higher degree of precision, the meshed domain consisting of a single entrance and a single exit has been investigated, as shown in Fig.9. Throughout the whole of this simulation, the velocity is maintained at a level that is quite similar to the real experimental velocity.

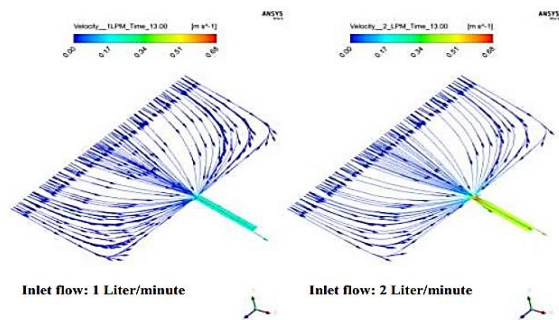


Fig. 9 Velocity vectors for the flow

Fig.9 illustrates the velocity vectors that may be found along the streamline of the water. The water travels at a sluggish pace in both of these instances (1 LPM and 2 Total Inlet flow: 1 Liter/minute), which is somewhere in the range of 0.03 to 0.06 metres per second. When the flow is getting close to the exit point, there is a dramatic increase in velocity for the 2 LPM flow; however, this increase happens extremely rapidly since it is so sudden. The PV panel temperature comparison with 1 LPM flow and 2 LPM flow can be seen in the snapshots in Fig.10A and Fig.10B, which were obtained at 10:00 and 13:00 hours, respectively. These

snapshots were taken at the same location as Fig.10A. According to the results of the simulation, a larger portion of the photovoltaic panel maintains a lower temperature when the flow rate is increased, and a higher flow rate is particularly required to keep the temperature stable when the intensity of the solar radiation is higher at 13:00 Hrs. As can be seen in Fig.11, when the panel's temperature is compared to the panel's temperature when cooling is not present, it is clear that the temperatures of the panel are well within the range in which they can be controlled with cooling.

When assessing the efficiency of PV panels, the V-I Performance measure is a useful tool to use. Fig.12 illustrates the efficiency of PV panels by drawing a comparison between the peak power provided by PV panels with and without cooling. This image also demonstrates how the performance of PV panels changes as they are being utilized.

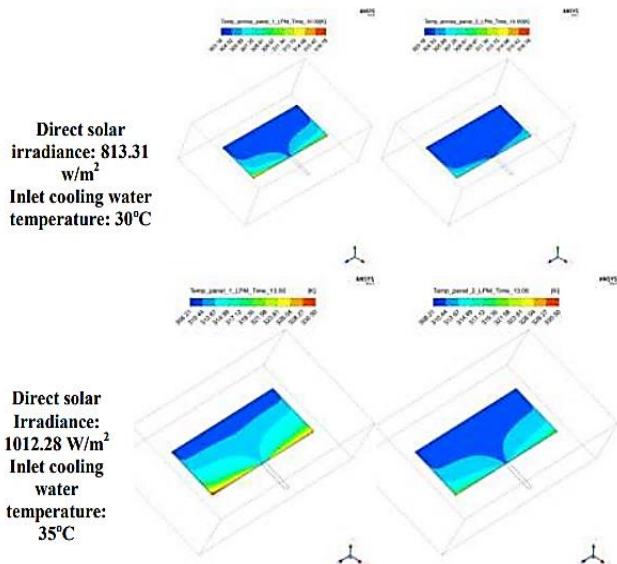


Fig. 10 PV panel temperature with cooling at 10:00 and 13:00, respectively, as shown in Fig.11 A (Top) and 11 B (Bottom).

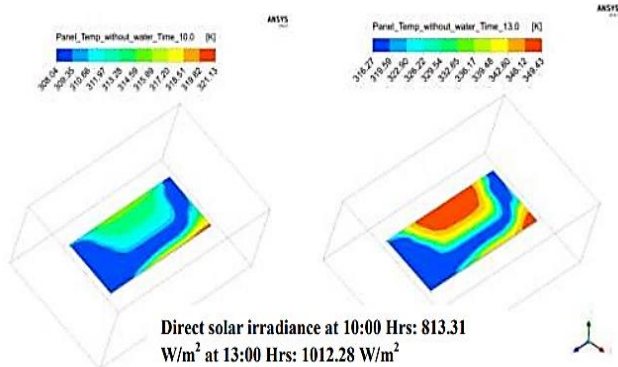


Fig. 11 Temperature of the panel without the use of cooling between 10:00 and 13:00 hours.

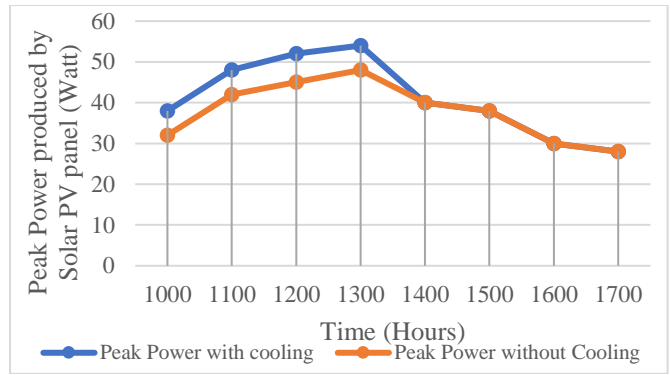


Fig. 12 Comparison of the performance of PV panels with and without cooling: 1 litre per minute of cooling water flow

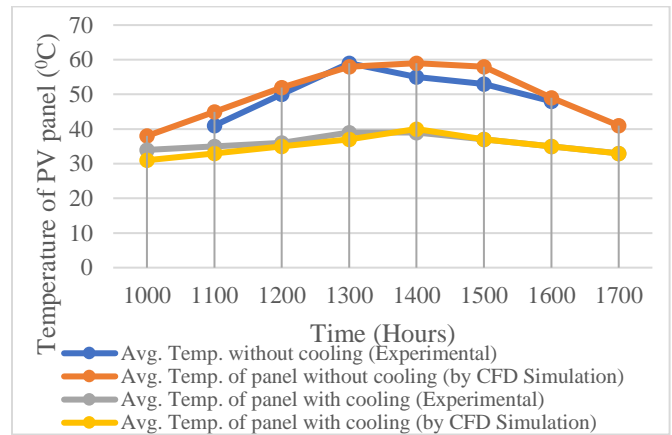


Fig. 13 Temperature of PV panel with and without cooling.

It is obvious that the peak power produced by PV panels rises with cooling, as demonstrated by the roughly 10 percent increase in power output observed at about 13:00 hours. This finding demonstrates the relationship between cooling and increased peak power generation. In order for the pump to function, it needs 5 W of power.

As a consequence of this, the quantity of net power produced by cooling has to be lowered by 5 W in each of the scenarios. On the other hand, gravity-operated devices can also be constructed so that the net power is equivalent to the generated power. This is called a "balanced system."

When cooling was used, a total of 333 watt-hours of energy was produced during the day. When cooling was not used, the total amount of energy produced was 303 watt-hours.

When there is a flow of 1 LPM, it is plainly obvious from Fig. 14 that there is a significant decrease in the temperature of the PV panel as a direct consequence of cooling from the top surface. This can be seen as a direct result of the cooling effect. When the findings of the experiment and the results of the CFD simulation are compared to one another, it is found that there is a strong similarity between the two sets of data. When there is no

cooling, the panel's temperature rises to somewhere close to 60 degrees celsius at about 14:00 hours. However, when there is cooling, the temperature is maintained at much below 40 degrees Celsius.

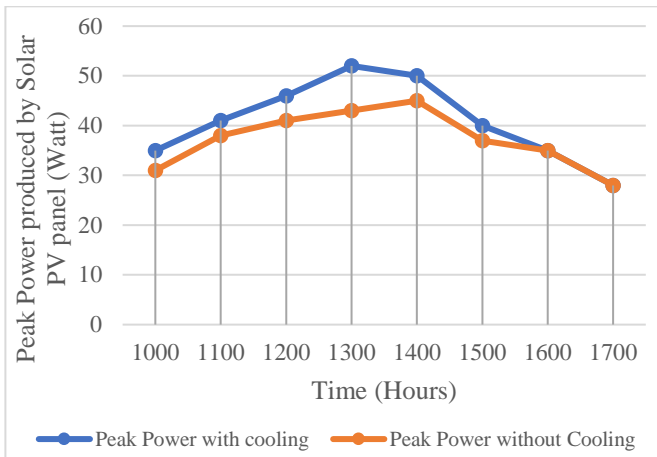


Fig. 14 A comparison of the efficiency of a photovoltaic panel with a cooling water flow of 2 LPM and one without cooling

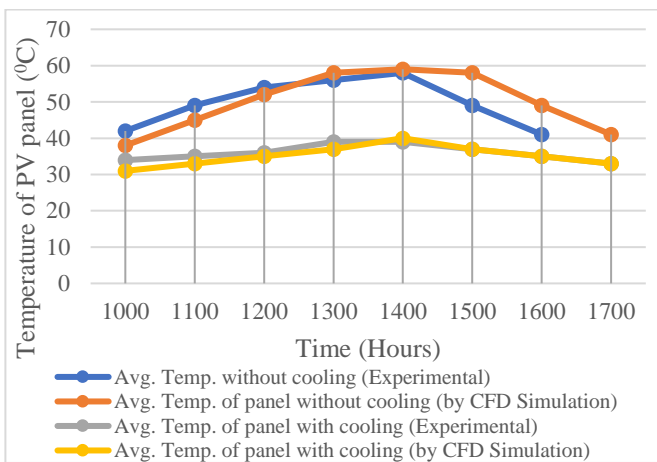


Fig. 15 Temperature of the photovoltaic panel with and without cooling -Cooling water flow of 2 LPM.

In contrast to the situation in which 1 LPM of flow was used, Fig. 14 shows that there is an increase in the peak power provided by the PV panel; despite this, the improvement is very considerable. As a consequence of recent advancements, the amount of peak power generated during the thirteen hours has grown by twenty percent. This gain has been placed over the course of the last several months.

The temperature of the photovoltaic panel drops from 58 degrees Celsius to 37 degrees Celsius when it is cooled with a flow of 2 litres per minute at 14:00 hours, as shown in Fig. 15. The image illustrates this drop-in temperature well. The experiment's findings and the conclusions taken from the simulation can be said to have a substantial degree of concordance with one another.

Table 2. The change in angle caused by the refraction caused by the solar PV panel

Time	Angle $\Theta_1$	Angle $\Theta_2$
09:00	-61.91	-41.58
10:00	-50.73	-35.63
11:00	-41.78	-30.09
12:00	-36.77	-26.76
13:00	37.27	27.10
14:00	43.11	30.94
15:00	52.54	36.66
16:00	63.98	42.53
17:00	76.49	47.00

It is obvious by looking at Table 2 that the incidence angle changed from -61.91 degrees to 76.49 degrees from 9:00 in the morning until 17:00 in the evening. After refraction, the angle shifts, and as a result, the value of angle (2) may range anywhere from -41.58 to 47.00.

In light of these findings, the experiment was carried out despite the fact that there was no justification for doing so. In both instances, the temperature of the photovoltaic panel was kept at 35 degrees Celsius by placing a layer of ice on the back of one panel and a layer of water that was exactly the same on top of the other panel. This was done in order to maintain the temperature of the panel. This was done in order to keep the temperature on both panels consistent with one another. However, the greatest power output measured while the water layer was on top was 54.04 Watt, but the highest power output recorded when the ice layer was on the bottom was only 50.22 watts. When the ice layer was on the bottom, the measurements were taken. Both measurements were taken at the exact same moment, which was thirteen o'clock in the morning. They were taken simultaneously (7.6 percent increase in power output). Because of this, it became abundantly evident that the refraction effect played a role in playing a role in contributing to the improvement of the panel's performance. Suppose there is an increase in the power production of around 20 percent in the majority of cases. In that case, the refraction effect may get credit for 7.6 percent of the credit, and cooling can receive credit for 12.4 percent of the credit. Overall efficiency in regard to the use of energy: In order to get a more in-depth grasp of the impact that cooling has on overall energy efficiency, a study was carried out that contrasted the levels of energy efficiency reached with and without the usage of cooling. As seen in Table 3, after the cooling operation was completed, there was a significant improvement in efficiency, which went from 6.68 percent to 40.42 percent. This was seen and noted.

With the cooling coming from the top in this manner, there is a considerable increase in the total energy efficiency (both thermal and electrical). Some processes, including reverse osmosis, need heated feed water, and this water may be utilized for such processes.

**Table 3. Calculations of energy efficiency (For 1 Liter/min flow)**

Time	12:00 Hrs.	14:00 Hrs.	16:00 Hrs.
Inlet water temp. ( $T_{w_{in}}$ )	37	36	34
Outlet water temp. ( $T_{w_{out}}$ )	39	38	35
Energy contained by water (watt)	139.5 6	139.5 6	69.78
Peak power without cooling (watt)	34.51	25.29	14.22
Peak power with cooling (watt)	41.73	28.57	16.3
Difference (watt)	7.22	3.28	2.08
Total power saving (watt)	146.7 9	142.8 5	71.86
Watt/m <sup>2</sup>	1020	732	348
Solar panel area (sq.m)	0.61	0.61	0.61
Power incident on the panel (watt)	624.2 4	447.9 8	212.9 8
Energy efficiency without cooling	5.53	5.64	6.68
Energy efficiency with cooling (Electrical + Thermal)	29.04	37.53	40.41

The increased permeability of the membrane caused by the higher temperature of the feed water allows for a greater quantity of product water to be produced from the same amount of membrane surface.

## 6. Conclusion

The performance of photovoltaic panels degrades with increasing temperatures; as a result, they need to be cooled to maintain or enhance their efficiency. The panel temperature

was effectively controlled by the transfer of heat from the top at a flow rate of just one to two litres per minute. Insulation on the back and sides of solar panels reduces heat loss as well as heat transmission from the bottom up. CFD analysis validates panel temperature studies. The beneficial refraction of solar radiation occurs when it strikes the water coating. Incoming radiation is narrowed across the panel as a result of refraction, which results in improved panel performance. The panel's power output is increased by water falling from the top of the panel. The increasing temperature of the water is consistent with the potential use of thermal energy. Distillation via membranes, reverse osmosis, and other processes may all benefit from water that has been heated to a higher temperature. The RO water flow may be increased by increasing temperature. Utilizing RO feed water as cooling water while simultaneously harvesting thermal energy as soon as possible is a really astute strategy. In order to optimize the energy efficiency of photovoltaic-powered reverse osmosis, it is feasible to use an interdisciplinary strategy that involves removing thermal energy from the solar panel while also preserving its temperature. The outcomes of this research indicate that raising the flow rate by one litre per minute and applying direct cooling to the surface of the PV panel array resulted in an improvement in the total energy efficiency of forty percent.

## Acknowledgment

The author would like to express gratitude to Professor Dr. Nilesh Diwakar of the Department of Mechanical Engineering, School of Engineering, SSSUTMS, Sehore, for serving as the research guide, as well as Professor Dr. Satish Chinchankar of the Department of Mechanical Engineering, VIIT, Pune, for serving as the co-guide for their technical assistance.

## References

- [1] Abdelrahman Aburub et al., "Experimental Investigations of a Cross-Flow Humidification Dehumidification Desalination System," *International Water Technology Journal*, vol. 7, no. 3, pp. 198-208, 2017. [[Google Scholar](#)]
- [2] Naseer Ahmad, "Modeling, Simulation and Performance Evaluation of a Community Scale PVRO Water Desalination System Operated by Fixed and Tracking PV Panels: A Case Study for Dhahran City, Saudi Arabia," *Renewable Energy*, vol. 75, pp. 433-447, 2015. [[CrossRef](#)] [[Google Scholar](#)] [[Publisher link](#)]
- [3] Kavita Joshi et al., "Maximum Power Operation of a PV System Employing Zeta Converter with Modified P&O Algorithm," *International Journal of Engineering Trends and Technology*, vol. 70, no. 7, pp. 348-354, 2022. [[CrossRef](#)] [[Publisher link](#)]
- [4] Farah Ejaz Ahmed, Raed Hashaikheh, and Nidal Hilal, "Solar-Powered Desalination-Technology, Energy and Future Outlook," *Desalination*, vol. 453, pp. 54-76, 2019. [[CrossRef](#)] [[Google Scholar](#)] [[Publisher link](#)]
- [5] M.A. Alghoul et al., "Design and Experimental Performance of Brackish Water Reverse Osmosis Desalination Unit Powered by 2 KW Photovoltaic System," *Renewable Energy*, vol. 93, pp. 101-114, 2016. [[CrossRef](#)] [[Google Scholar](#)] [[Publisher link](#)]
- [6] Kyaw Thu, Yin Maung Maung, and Than Than Win, "Modelling of a Solar Cell Considering Single-Diode Equivalent Circuit Using Matlab/Simulink," *SSRG International Journal of Electronics and Communication Engineering*, vol. 6, no. 6, pp. 5-9, 2019. [[CrossRef](#)] [[Publisher link](#)]
- [7] Ehab S. Ali, "Recycling Brine Water of Reverse Osmosis Desalination Employing Adsorption Desalination: A Theoretical Simulation," *Desalination*, vol. 408, pp. 13-24, 2017. [[CrossRef](#)] [[Google Scholar](#)] [[Publisher link](#)]
- [8] Arvind Prabhakar, "CFD Analysis of Static Pressure and Dynamic Pressure for NACA 4412," *International Journal of Engineering Trends and Technology*, vol. 4, no. 8, 2013. [[Google Scholar](#)] [[Publisher link](#)]

- [9] Ines Ben Ali, "Systemic Design of a Reverse Osmosis Desalination Process Powered by Hybrid Energy System," *International Conference on Electrical Sciences and Technologies in Maghreb (CISTEM)*, pp. 1-6, 2014. [[CrossRef](#)] [[Google Scholar](#)] [[Publisher link](#)]
- [10] Mahalakshmaiah Vaddani Dr.V.Krishnareddy, "CFD Analysis of Variable Helical Inlet Port for a Six Cylinder Engine," *SSRG International Journal of Mechanical Engineering*, vol. 1, no. 6, pp. 16-21, 2014. [[CrossRef](#)] [[Publisher link](#)]
- [11] Mohamed A. Antar, and Mostafa H. Sharqawy, "Experimental Investigations on the Performance of an Air Heated Humidification–Dehumidification Desalination System," *Desalination and Water Treatment*, vol. 51, no. (4-6), pp. 837-843, 2012. [[CrossRef](#)] [[Google Scholar](#)] [[Publisher link](#)]
- [12] Pınar İlker Ayav, and Gürbüz Atagündüz, "Theoretical and Experimental Investigations on Solar Distillation of IZTECH Campus Area Seawater," *Desalination*, vol. 208, no. 1-3, pp. 169-180. [[CrossRef](#)] [[Google Scholar](#)] [[Publisher link](#)]
- [13] Jasminder Singh et al., "Study of NACA 4412 and Selig 1223 Airfoils Through Computational Fluid Dynamics," *SSRG International Journal of Mechanical Engineering*, vol. 2, no. 6, pp. 17-21, 2015. [[CrossRef](#)] [[Google Scholar](#)] [[Publisher link](#)]
- [14] Sachankar Buragohain, Kaustubha Mohanty, and Pinakeswar Mahanta, "Experimental Investigations of a 1 Kw Solar Photovoltaic Plant in Standalone and Grid Mode at Different Loading Conditions," *Sustainable Energy Technologies and Assessments*, vol. 41, p. 100796, 2020. [[CrossRef](#)] [[Google Scholar](#)] [[Publisher link](#)]
- [15] Alper BURGAÇ, and Hakan Yavuz, "Examination of Desalination Model Parameters on a Reverse Osmosis Desalination Simulation Model," *Bilecik Şeyh Edebali University Journal of Science*, vol. 8, no. 2, pp. 614-621, 2021. [[CrossRef](#)] [[Google Scholar](#)] [[Publisher link](#)]
- [16] Snehal C. Kapse, and Dr. R.R Arakerimath, "CFD Analysis & Optimisation Parametric Study on Heat Transfer Enhancement by Various Shapes of Wings and Materials with Forced Convection," *SSRG International Journal of Mechanical Engineering*, vol. 1, no. 8, pp. 1-3, 2014. [[CrossRef](#)] [[Google Scholar](#)] [[Publisher link](#)]
- [17] A.B. Chaaben et al., "MIMO Modeling Approach for a Small Photovoltaic Reverse Osmosis Desalination System," *Journal of Applied Fluid Mechanics*, vol. 4, no. 1, pp. 35-41, 2012. [[CrossRef](#)] [[Google Scholar](#)] [[Publisher link](#)]
- [18] Rym Chaker et al., "A Trnsys Dynamic Simulation Model for Photovoltaic System Powering a Reverse Osmosis Desalination Unit with Solar Energy," *International Journal of Chemical Reactor Engineering*, vol. 8, no. 1, 2010. [[CrossRef](#)] [[Google Scholar](#)] [[Publisher link](#)]
- [19] Asem Al Jarrah, "CFD Study of the Normal Force Exerted on a Sphere Moving Close to a Surface," *SSRG International Journal of Chemical Engineering Research*, vol. 3, no. 1, pp. 1-6, 2016. [[CrossRef](#)] [[Publisher link](#)]
- [20] Chao Chen, "Sustainably Integrating Desalination with Solar Power to Overcome Future Freshwater Scarcity in China," *Global Energy Interconnection*, vol. 2, no. 2, pp. 98-113, 2019. [[CrossRef](#)] [[Google Scholar](#)] [[Publisher link](#)]
- [21] Habib Cherif, "Large-Scale Time Evaluation for Energy Estimation of Stand-Alone Hybrid Photovoltaic–Wind System Feeding a Reverse Osmosis Desalination Unit," *Energy*, vol. 36, no. 10, pp. 6058-6067, 2011. [[CrossRef](#)] [[Google Scholar](#)] [[Publisher link](#)]
- [22] Gadadhe, Shivaji S et al., "A Survey on Experimental Investigations and Simulation on Solar Powered Reverse Osmosis Water Desalination System," *International Journal of Mechanical Engineering*, vol. 6, no. 3, pp. 2753-2765, 2021. [[Google Scholar](#)]